DR. LYLE A SIMMONS (Orcid ID : 0000-0002-9600-7623)



Article type : Research Article

# A bacterial DNA repair pathway specific to a natural antibiotic

Peter E. Burby and Lyle A. Simmons*

Department of Molecular, Cellular, and Developmental Biology, University of Michigan, Ann Arbor, MI 48109, United States.

*Corresponding author

LAS: Department of Molecular, Cellular, and Developmental Biology, University of Michigan, Ann Arbor, Michigan 48109-1055, United States. Phone: (734) 763-7142, Fax: (734) 647-0884

E-mail: lasimm@umich.edu

Running Title: MrfAB are a novel excision repair pathway

Key words: Mitomycin C, DNA repair, helicase, exonuclease.

## Summary

All organisms possess DNA repair pathways that are used to maintain the integrity of their genetic material. Although many DNA repair pathways are well understood, new pathways continue to be discovered. Here, we report an antibiotic specific DNA repair pathway in *Bacillus subtilis* that is composed of a previously uncharacterized helicase (*mrfA*) and exonuclease (*mrfB*). Deletion of *mrfA* and *mrfB* results in sensitivity to the DNA damaging agent mitomycin C, but not to any other type of DNA damage tested. We show that MrfAB function independent of canonical nucleotide excision repair, forming a novel excision repair pathway. We demonstrate that MrfB is a metal-dependent exonuclease and that the N-terminus of MrfB is required for interaction with MrfA. We determined that MrfAB failed to unhook inter-strand crosslinks *in vivo*, suggesting that MrfAB are specific to the monoadduct or the intra-strand crosslink. A phylogenetic analysis uncovered MrfAB homologs in diverse bacterial phyla, and cross-complementation indicates that MrfAB function is conserved in closely related species. *B. subtilis* is a soil dwelling organism and mitomycin C is a natural antibiotic produced by the soil bacterium *Streptomyces lavendulae*. The specificity of MrfAB suggests that these proteins are an adaptation to environments with mitomycin producing bacteria.

## Abbreviated Summary

Bacteria possess DNA repair pathways to maintain the integrity of their genetic material. The putative helicase MrfA and the exonuclease MrfB are part of a mitomycin C (MMC) specific DNA repair pathway in *Bacillus subtilis*. Despite being present in many bacterial species, MrfAB activity in repairing MMC damaged DNA appears to be restricted to closely related species, suggesting that despite sequence conservation these proteins have evolved to the specific repair needs of each bacterium.

## Introduction

A defining feature of biology is the ability to reproduce, which requires replication of the genetic material. High fidelity DNA replication depends on the integrity of the template DNA which can

be damaged by UV light, ionizing radiation, and numerous chemicals (Friedberg et al., 2006). Many DNA damaging agents have been used as chemotherapeutics and are also produced from natural sources such as bacteria, fungi, or plants (Demain & Vaishnav, 2011). One such naturally produced antibiotic is mitomycin C (MMC), originally isolated from *Streptomyces lavendulae* (Hata et al., 1956). MMC is produced as an inactive metabolite that must be activated by enzymatic or chemical reduction to react with DNA (Tomasz, 1995). MMC reacts specifically with guanine residues in DNA and results in three principle modifications (Bargonetti, Champeil, & Tomasz, 2010). MMC forms a mono-adduct by reacting with a single guanine, however, MMC has two reactive centers, which can result in intra-strand crosslinks on adjacent guanines on the same strand, or in inter-strand crosslinks wherein the two guanines on opposite strands of CpG sequences are covalently linked (Bizanek, McGuinness, Nakanishi, & Tomasz, 1992; Borowyborowski, Lipman, Chowdary, & Tomasz, 1990; Borowyborowski, Lipman, & Tomasz, 1990; Iyer & Szybalski, 1963; Kumar, Lipman, & Tomasz, 1992; Tomasz et al., 1986; Tomasz et al., 1987). The toxicity of these different adducts is a result of preventing DNA synthesis (Bargonetti et al., 2010).

In bacteria, MMC adducts and intra-strand crosslinks are repaired by nucleotide excision repair and inter-strand crosslinks are repaired by a combination of nucleotide excision repair and homologous recombination (Dronkert & Kanaar, 2001; Lenhart, Schroeder, Walsh, & Simmons, 2012; Noll, Mason, & Miller, 2006). Both mono-adducts and crosslinks are recognized in genomic DNA by UvrA to initiate repair (Jaciuk, Nowak, Skowronek, Tanska, & Nowotny, 2011; Kisker, Kuper, & Van Houten, 2013; Stracy et al., 2016; Weng et al., 2010). In some nucleotide excision repair models UvrB functions in complex with UvrA (Kisker et al., 2013; Truglio, Croteau, Van Houten, & Kisker, 2006; Van Houten, Croteau, DellaVecchia, Wang, & Kisker, 2005), while *in vitro* studies and a recent *in vivo* study using single molecule microscopy suggests that UvrB is recruited by UvrA (Orren & Sancar, 1989; Stracy et al., 2016). In any event, once UvrA and UvrB are present at the lesion, the subsequent step is the disassociation of UvrA and the recruitment of UvrC which incises the DNA on either side of the lesion (Orren & Sancar, 1989).

In *E. coli* there is a second UvrC-like protein called Cho that can also perform the incision function (Moolenaar, van Rossum-Fikkert, van Kesteren, & Goosen, 2002; Perera,

Mendenhall, Courcelle, & Courcelle, 2016). Mono-adducts and intra-strand crosslinks are removed from the DNA via UvrD helicase in *E. coli* after UvrC excision. The resulting single-stranded gap is resynthesized by DNA polymerase with DNA ligase sealing the remaining nick, completing the repair process (Kisker et al., 2013; Petit & Sancar, 1999). For an inter-strand crosslink, the process requires another step because the lesion containing DNA remains covalently bonded to the opposite strand. Most current models propose that homologous recombination acts subsequently to pair the lesion containing strand with a second copy of the chromosome if present and then an additional round of nucleotide excision repair can remove the crosslink followed by DNA polymerase and DNA ligase to complete the repair process (Dronkert & Kanaar, 2001; Noll et al., 2006). Importantly, homologous recombination and UvrABC-dependent nucleotide excision repair are general DNA repair pathways that participate in the repair of many different types of DNA lesions including MMC adducted DNA.

Although the pathways discussed above are known to function in the repair of MMC damaged DNA, it is unclear if other pathways exist in bacteria that also repair MMC lesions. We recently reported a forward genetic screen in *B. subtilis* where we identified two genes, *mrfA* and *mrfB* (formerly *yprA* and *yprB*, respectively) that when deleted resulted in sensitivity to MMC (Burby, Simmons, Schroeder, & Simmons, 2018). Here, we report that MrfAB are part of a MMC specific DNA repair pathway in *B. subtilis*. Deletion of the *mrfAB* (formerly *yprAB*) operon renders *B. subtilis* sensitive to MMC, but not to other DNA damaging agents known to be repaired by the canonical nucleotide excision repair pathway. MrfAB are a putative helicase and exonuclease, respectively, and we demonstrate that conserved residues required for their activities are important for function *in vivo*. We show that MrfAB operate independent of UvrABC. We monitored DNA repair status over time using RecA-GFP as a reporter, and we show that deletion of *mrfAB* and *uvrABC* results in a synergistic decrease in RecA-GFP foci, suggesting that MrfAB are part of a novel nucleotide excision repair pathway in bacteria. We also found that MrfAB do not contribute to inter-strand crosslink repair, suggesting that MrfAB are specific to MMC mono-adducts or intra-strand crosslinks. A phylogenetic analysis shows that MrfAB homologs are present in many bacterial species and that the function of MrfAB is conserved in closely related species. Together, our study identifies a novel strategy used by bacteria to counteract the natural antibiotic MMC.

## Results

### DNA damage sensitivity of Δ*mrfAB* is specific to mitomycin C

Our recent study using a forward genetic screen identified genes important for surviving exposure to several DNA damaging agents, uncovering many genes that had not previously been implicated in DNA repair or regulation of the SOS-response (Burby et al., 2018). As part of this screen, we identified a gene pair, *yprAB*, in which disruption by a transposon resulted in sensitivity to MMC but not phleomycin or methyl methanesulfonate (Fig 1A) (Burby et al., 2018). Because the phenotypes appeared specific to MMC (see below), we rename *yprAB* to mitomycin repair factors A and B (*mrfAB*). To follow up on the phenotype of the transposon insertions we tested clean deletion strains of *mrfA* and *mrfB* and found that deletion of either gene resulted in sensitivity to MMC (Fig 1B). Further, we ectopically expressed each gene in its respective deletion background and were able to complement the MMC sensitive phenotype (Fig 1B).

The absence of phenotypes with phleomycin and methyl methanesulfonate, is similar to the phenotypic profile of nucleotide excision repair (NER) mutants (Fig 1A) (Burby et al., 2018). Therefore, we asked if deletion of *mrfA* would result in sensitivity to other agents known to be repaired by NER. We tested for sensitivity to three other agents that cause DNA lesions that are repaired by NER: UV light, 4-NQO, and the DNA crosslinking agent psoralen (trioxsalen) (Petit & Sancar, 1999). Interestingly, we found that deletion of *mrfA* did not cause sensitivity to any of these agents (Fig 1C). We also tested whether the presence of *uvrAB* was masking the effect, but no additional sensitivity was observed when *mrfA* was deleted in the Δ*uvrAB* background (Fig 1C). Given the absence of phenotypes to other DNA damaging agents, MrfAB do not function as a general nucleotide excision repair pathway. In addition, *mrfAB* deletion did not result in sensitivity to another crosslinking agent, psoralen, indicating that MrfAB are not part of a general crosslink repair mechanism. We conclude that MrfAB are important for mitigating the toxicity of MMC-generated DNA lesions.

### MrfA and MrfB function in the same pathway

The phenotypes of *mrfA* and *mrfB* mutants were identical (Fig 1A & B), and the two genes are predicted to be an operon. Therefore, we hypothesized that MrfA and MrfB likely function

together. We tested this hypothesis by combining the deletion mutants. We found that deletion of both genes gave the same sensitivity to MMC as each single mutant (Fig 2A), indicating that they function in the same pathway. If MrfAB function in the same pathway, it is possible that each protein acts successively, MrfA and MrfB interact forming a complex, or one protein serves to recruit the other in a stepwise fashion.

To provide insight into these possible mechanisms we tested for a protein-protein interaction between MrfA and MrfB using a bacterial two-hybrid assay (Karimova, Gauliard, Davi, Ouellette, & Ladant, 2017; Karimova, Pidoux, Ullmann, & Ladant, 1998). We found that MrfA and MrfB formed a robust interaction, indicated by the formation of blue colonies (Fig 2B). Next, we wanted to understand how these proteins interacted and whether we could localize the interaction to a particular domain. We performed a deletion analysis with MrfA and found that deletion of either the N-terminus or the C-terminus was sufficient to abolish the interaction with MrfB (Fig 2C), and the N-terminus of MrfA was not sufficient for MrfB interaction (Fig 2C). Thus, it appears that the portion of MrfA that is required for the interaction is not limited to a single domain. We tested whether the N-terminus or C-terminus of MrfB was required for MrfA interaction. We found that the C-terminus of MrfB was not required, though the signal was reduced, whereas deletion of the N-terminus of MrfB abolished the interaction with MrfA (Fig 2D). Therefore, the N-terminus of MrfB is required for interaction with MrfA. We conclude that MrfAB interaction is specific and that these proteins function as a complex or one protein subsequently recruits the other.

**MrfA helicase motifs and C-terminus is required for function *in vivo***

MrfA is a predicted DEXH box helicase containing a C-terminal domain of unknown function (Fig S1 and S2A). The C-terminal domain of unknown function contains four conserved cysteines that are thought to function in coordinating a metal ion (Shi et al., 2011; Yakovleva & Shuman, 2012). We initially searched for a similar helicase in other well studied organisms. We were unable to identify a homolog of MrfA containing both the ATPase domain and the C-terminal domain in *E. coli*, however, Hrq1 from *Saccharomyces cerevisiae* shares the same domain structure with 32% identity and 55% positives. Hrq1 has been shown to be a RecQ family helicase with 3′→ 5′ helicase activity and has been observed to exist as a heptamer (Bochman, Paeschke, Chan, & Zakian, 2014; Rogers et al., 2017). We performed an alignment

with Hrq1 and identified helicase motifs typical of super family 2 helicases (Fig S1). A homolog of MrfA from *Mycobacterium smegmatis* has also been shown to be a 3′→ 5′ helicase, however, unlike Hrq1, SftH exists as a monomer in solution (Yakovleva & Shuman, 2012).

To address whether residues predicted to be important for MrfA helicase activity are required for function, we used a complementation assay using variants containing alanine substitutions in several conserved helicase motifs. Mutations in helicase motif I (K82A), motif II (DE185-186AA), and motif III (S222A) all failed to complement a *mrfA* deficiency (Fig S2B). Intriguingly, when motif Ib (T134V) was mutated *mrfA* MMC sensitivity could still be complemented, and this residue, although conserved in Hrq1, it is not conserved in SftH (Fig S2B). We asked whether the C-terminal domain of unknown function and the conserved cysteines were required for function. Deletion of the entire C-terminal domain, mutation of the first two cysteines, or mutation of all four cysteines all resulted in a failure to complement MMC sensitivity in a Δ*mrfA* strain (Fig S2B). Together with our data we suggest that both the putative helicase domain and the C-terminal domain of unknown function are required for MrfA *in vivo*.

**MrfB is a metal-dependent exonuclease**

MrfB is predicted to be a DnaQ-like exonuclease and to have three tetratrichopeptide repeats at the C-terminus (Fig 3A). To search for putative catalytic residues in MrfB, we aligned MrfB to ExoI, ExoX, and DnaQ from *E. coli* (Fig S3A). MrfB has the four acidic residues typical of DnaQ-like exonucleases (Fig S3A). This type of nuclease also has a histidine located proximal to the last aspartate (Yang, 2011), and we identified two histidine residues, one of which was conserved (Fig S3A, conserved histidine highlighted in red and the other in green). DnaQ exonucleases coordinate a metal ion that is used in catalysis (Yang, 2011). We hypothesized that MrfB catalytic residues would cluster together in the tertiary structure. We modelled MrfB using Phyre2.0 (Kelley, Mezulis, Yates, Wass, & Sternberg, 2015), which used DNA polymerase epsilon catalytic subunit A (DnaQ) [pdb structure c5okiA (Grabarczyk, Silkenat, & Kisker, 2018)], and show that the conserved aspartate and glutamate residues are indeed clustered together in the model (Fig S3B).

Interestingly, we found that the histidine conserved in the *E. coli* exonucleases was facing the opposite direction, whereas the non-conserved histidine was facing the putative catalytic

residues in the MrfB model (Fig S3C). An alignment of MrfB homologs demonstrates that the histidine (labeled in green) facing the other putative catalytic residues is conserved in MrfB homologs, whereas the other is not (see supplemental text). To test whether these residues were important for function, we used variants with alanine substitutions at each putative catalytic residue in a complementation assay. We found that all five mutants could not complement the Δ*mrfB* mutant phenotype (Fig 3B).

With these results we wanted to test whether MrfB had exonuclease activity *in vitro*. We overexpressed and purified MrfB to homogeneity as determined by SDS-PAGE (Fig 3C). We tested for exonuclease activity using a plasmid linearized by restriction digest. We found that MrfB could degrade linear dsDNA in the presence of $Mg^{2+}$, demonstrating that MrfB is a metal-dependent exonuclease (Fig 3D). With exonuclease activity established we tested the substrate preference of MrfB using a closed circular covalent plasmid (CCC), a nicked plasmid or a linear plasmid using $T_5$ and λ exonucleases as controls. $T_5$ exonuclease is able to degrade both nicked and linear substrates but $T_5$ cannot degrade a CCC plasmid (Sayers & Eckstein, 1990, 1991). In contrast, λ exonuclease can only degrade a linear substrate (Little, 1981). The $T_5$ and λ exonuclease controls performed as predicted, and MrfB demonstrated activity on a linear substrate and lower activity using a nicked substrate (Fig 3E). We conclude that MrfB is a metal-dependent exonuclease with a preference for linear DNA.

**MrfAB function independent of UvrABC dependent nucleotide excision repair**

Given that DNA damage sensitivity in *mrfAB* mutants was restricted to MMC and that both proteins have nucleic acid processing activities, we hypothesized that MrfAB were part of a nucleotide excision repair pathway. We tested whether MrfAB were within the canonical, UvrABC-dependent nucleotide excision repair pathway using an epistasis analysis. We found that deletion of *mrfA* or *mrfB* rendered *B. subtilis* hypersensitive to MMC in the absence of *uvrAB* (Fig 4A), *uvrC*, or *uvrABC* (Fig 4B). We also show that *uvrABC* function as a single pathway showing that deletion of each gene resulted in the same phenotype as the triple deletion (Fig S4). It is important to note that *B. subtilis uvrABC* functioning as a single pathway differs from *E. coli* (Lage, Goncalves, Souza, de Padula, & Leitao, 2010; Perera et al., 2016).

To test whether deletion of *mrfAB* have an effect on acute treatment with MMC, we performed an epistasis analysis using a MMC survival assay. We tested mutants in *mrfAB*, *uvrABC*, and the double pathway mutant. We found that deletion of *mrfAB* had a limited, yet statistically significant (Mann-Whitney U-test; p-value < 0.05) effect on acute sensitivity to MMC at the 150 and 200 ng/mL treatments. Deletion of *uvrABC* had a significant and more pronounced decrease in survival following MMC treatment (Fig 4C). Deletion of both pathways resulted in hypersensitivity to acute MMC exposure, suggesting that MrfAB are part of a second nucleotide excision repair pathway. The difference in phenotypes between the individual pathway mutants suggests that the roles of each pathway may be specific for different MMC induced lesions. Given that the inter-strand crosslink is the more toxic lesion, our data suggest that UvrABC could be more efficient for repair of crosslinks and MrfAB could be more specific to the mono-adducted lesions (see below). We conclude that MrfAB and UvrABC are part of two distinct pathways for MMC repair.

**MrfAB are not required for unhooking inter-strand DNA crosslinks**

As stated previously, MMC results in several DNA lesions, one of which is the inter-strand crosslink. Our results from treating acutely with MMC suggested that MrfAB may not function in repair of the inter-strand crosslink. Therefore, we asked whether one or both pathways contribute to unhooking DNA crosslinks *in vivo*. Crosslinked DNA can be detected by heat denaturing and snap cooling due to the fact that crosslinked DNA will renature during the rapid cooling process and DNA that is not crosslinked will remain denatured when cooled rapidly (Iyer & Szybalski, 1963). Therefore, we hypothesized that if both pathways contributed to unhooking a crosslink, we would observe stable DNA crosslinks only in the double pathway mutant. If only a single pathway was required, we would observe stable DNA crosslinks in one mutant and the double pathway mutant background. To test these ideas, we treated *B. subtilis* strains with MMC to crosslink genomic DNA, and then allowed the cells to recover for 45 or 90 minutes. We monitored DNA crosslinks by denaturing and snap cooling the DNA followed by analysis on an agarose gel. We found that in WT and Δ*mrfAB* cells we could detect some crosslinked DNA that decreased slightly over time (Fig 5A). Additionally, at the 90 minute recovery time point we observed a smaller DNA fragment in WT and Δ*mrfAB* samples, which we suggest is a result of a repair intermediate generated by UvrABC-dependent incision because formation of the

intermediate requires UvrABC (Fig 5A). In the absence of *uvrABC* there was a significant stabilization of crosslinked DNA that did not decrease over time and deleting *mrfAB* had no effect in the *uvrABC* mutant strain on crosslink stabilization (Fig 5A). We quantified the crosslinked species and found that the inter-strand crosslink was stabilized in the absence of *uvrABC* and in the double pathway mutant (Fig 5B). We conclude that UvrABC are the primary proteins responsible for repair of inter-strand crosslinks and MrfAB likely repair the more abundant mono-adducts (Warren, Maccubbin, & Hamilton, 1998) and potentially intra-strand crosslinks that form, though we cannot formerly exclude the possibility that MrfAB act on an intermediate of the crosslink repair pathway that is specific to MMC.

**MrfAB and UvrABC are required for efficient RecA-GFP focus formation**

The synergistic sensitivity to MMC observed in the double pathway mutant suggests that MrfAB are part of a novel nucleotide excision repair pathway that does not function in inter-strand crosslink repair. Thus, we sought to determine if DNA repair is altered following MMC treatment in the absence of *mrfAB*. Previous studies have demonstrated that RecA-GFP forms foci in response to DNA damage such as treatment with MMC (Kidane & Graumann, 2005; Simmons et al., 2009; Simmons, Grossman, & Walker, 2007). Additionally, the activation of the SOS response following treatment with MMC in bacteria requires the generation of a RecA/ssDNA nucleoprotein filament (Kreuzer, 2013), which was also found to depend on nucleotide excision repair (Sassanfar & Roberts, 1990). Therefore, to test whether the response of RecA was affected by the absence of *mrfAB*, *uvrABC*, or both pathways, we used a RecA-GFP fusion as a reporter to monitor RecA status over time (Fig 6A & S5). We quantified the percentage of cells containing a focus or foci of RecA-GFP, and found an increase in RecA-GFP focus formation over time (Fig 6B). In all three mutant strains there was a significant increase in RecA-GFP foci prior to MMC addition (Fig 6B). We found that deletion of *mrfAB* did not have a significant impact on RecA-GFP focus formation (Fig 6B). Deletion of *uvrABC* led to a slight decrease in RecA-GFP focus formation (Fig 6B & S5). The double pathway mutant had a significant decrease in RecA-GFP foci relative to WT (Fig 6B). With these results we suggest that RecA is responding to excision repair gaps that occur after removal of the MMC adduct and that the RecA response is substantially decreased in cells that lack the excision activity of

*uvrABC* and *mrfAB*. These results further support the conclusion that MrfAB participate in the repair of MMC damaged DNA.

**MrfAB are conserved in diverse bacterial phyla**

Given the specificity of MrfAB for MMC, we became interested in understanding how conserved *mrfA* and *mrfB* are across different bacterial phyla. We performed a PSI-BLAST search using MrfA or MrfB against the proteomes of bacterial organisms from several phyla (Fig 7A; Table S4). We found that MrfA and MrfB are both present in organisms from 5 different phyla, though MrfA is more broadly conserved in bacteria (Fig 7A). To test if MrfA and MrfB function is conserved, we attempted to complement the MMC sensitive phenotype using codon-optimized versions of the homologs from three organisms, *Bacillus cereus*, *Streptococcus pneumoniae*, and *Pseudomonas aeruginosa*. We found that expression of *Bc-mrfA* and *Bc-mrfB* were capable of complementing their respective deletions (Fig 7B). Interestingly, *Sp-mrfB* complemented, but *Sp-mrfA* did not (Fig 7B). The more distantly related homologs from *P. aeruginosa* were not able to complement the corresponding deletion alleles (Fig 7B). We conclude that MrfA and MrfB function is conserved in closely related species, and that they likely have been adapted to other uses in more distantly related bacteria.

## Discussion

MrfAB are founding members of a novel bacterial nucleotide excision repair pathway. The observation that RecA-GFP foci changes in a synergistic manner with deletion of both *uvrABC* and *mrfAB* suggests that MrfAB are acting as a second excision repair pathway leaving a gap. Indeed, a study of SOS activation in *E. coli* found that deletion of *uvrA* results in decreased SOS response activation when treated with MMC (Sassanfar & Roberts, 1990). The activation of the SOS response requires the formation of the RecA/ssDNA nucleoprotein filament that can be observed *in vivo* using a RecA-GFP fusion (Ivancic-Bace, Vlasic, Salaj-Smic, & Brcic-Kostic, 2006; Lenhart et al., 2014; Simmons, Foti, Cohen, & Walker, 2008; Simmons et al., 2009; Simmons et al., 2007). Thus, our data are supportive of the excision repair model. We cannot formerly exclude the possibility that MrfAB act on a DNA repair intermediate, however, given that the *mrfAB* deletion did not render cells sensitive to other DNA damaging agents, this intermediate would have to be specific to the repair of MMC generated lesions.

Our current model is that a MMC mono-adduct or intra-strand crosslink is recognized by MrfA or an unknown factor (Fig 8). After the lesion is recognized it is possible that incisions occur on either side of the lesion or a single incision is used. It is also possible that no incision is required and that MrfAB make use of transient nicks in the chromosome that would be present during synthesis of the lagging strand, though this model would limit the lesions that MrfAB could repair. Once a nick is present, we hypothesize that MrfA acts as helicase to separate the DNA, exposing the MMC lesion. If a nick is generated 3′ to the lesion, MrfA could access the DNA at the nick and use its putative 3′→5′ helicase activity to separate the lesion containing strand for degradation by MrfB (Fig 8). If MrfA made use of transient nicks in the chromosome generated during lagging strand synthesis, then it is possible that MrfA could recognize or be recruited to the MMC lesion and use its 3′→5′ helicase activity on the strand opposite the lesion thereby exposing the lesion containing strand which could be stabilized by SSB, and upon reaching the nick in the DNA strand containing the lesion, MrfB could access the 3′ end to degrade the lesion containing strand. Our data cannot distinguish between these models, however, the Hrq1 and SftH have been observed to require a 3′ tail for helicase activity (Bochman et al., 2014; Kwon, Choi, Lee, & Bae, 2012; Rogers & Bochman, 2017; Yakovleva & Shuman, 2012). Therefore, we hypothesize that a 3′ tail is necessary after lesion recognition, to allow for MrfA to separate the lesion containing strand.

The specificity of the Δ*mrfAB* phenotype suggests that lesion recognition depends on MMC adduct structure. Our reported screen did not identify other candidates for this pathway (Burby et al., 2018) , though it remains possible that an essential protein or a protein that functions in homologous recombination, which would have a more severe phenotype than *mrfAB*, also acts as a lesion recognition factor. Nonetheless, we hypothesize that lesion recognition is a function accomplished by either MrfA, MrfB, or by both proteins in complex. MrfA is a putative helicase with a C-terminal domain of unknown function containing four well conserved cysteine residues. A high throughput X-ray absorption spectroscopy study of over 3000 proteins including MrfA reported finding that MrfA binds zinc (Shi et al., 2011). Intriguingly, UvrA, the recognition factor of canonical nucleotide excision repair, also contains a zinc finger which is required for regulating recognition of damaged DNA (Croteau et al., 2006). Indeed, three of the four recognition factors in eukaryotic nucleotide excision repair, XPA, RPA, and TFIIH also each contain a zinc finger component (Petit & Sancar, 1999). Therefore, it is

tempting to speculate that MrfA functions as the lesion recognition factor through its putative C-terminal zinc finger domain.

The initial finding that sensitivity to DNA damage in *mrfAB* mutants is specific to MMC suggested an antibiotic specific repair pathway. The major source of toxicity from MMC has long been thought to be the inter-strand crosslink (Bargonetti et al., 2010). We found that MrfAB do not contribute to unhooking an inter-strand crosslink *in vivo* and yet deletion of *mrfAB* in the *uvrABC* mutant resulted in a significant decrease in survival following MMC treatment. With these observations we strongly suggest that the mono-adducts and/or the intra-strand crosslink make a significant contribution to the overall toxicity of MMC. Therefore, through identifying a new repair pathway in bacteria, we are able to provide new insight into the toxicity profile of a well-studied, natural antibiotic.

MrfAB homologs have likely evolved to perform different functions depending on the environments of their respective bacterial species, despite significant sequence similarity. We speculate that MrfAB specificity for MMC is a reflection of habitat overlap between *B. subtilis* and mitomycin producing bacteria such as *S. lavendulae*. Thus, MrfAB are an adaptation that allows *B. subtilis* to effectively compete in habitats where MMC is produced. Given that only closely related species could substitute for MrfA and MrfB in *B. subtilis*, we hypothesize that the MMC specific repair activity is restricted to those species. In fact, the homologs present in *P. aeruginosa* have diverged significantly (Table S4). The N-terminus of *Pa*-MrfA is quite different from that of *Bs*-MrfA, and the C-terminal TPR domain of MrfB is completely absent in *Pa*-MrfB (see supplemental alignments), consistent with the notion that MrfAB function has diverged in more distantly related bacteria. Additionally, our results with MrfAB from *S. pneumoniae* are supportive of our hypothesis that MrfAB function in MMC repair is restricted to closely related organisms. We speculate the interaction between *Sp*-MrfA and *Sp*-MrfB is conserved such that *Sp*-MrfB can still be recruited by *Bs*-MrfA and MrfB retains exonuclease activity, while the function of *Sp*-MrfA has diverged and the lesion recognition or recruitment activity is no longer present.

We recently investigated the mismatch repair homolog MutS2 and arrived at a similar conclusion—MutS2 has been adapted to the specific DNA repair needs of different organisms. MutS2 in *B. subtilis* promotes homologous recombination (Burby & Simmons, 2017), whereas

MutS2 in several other organisms inhibits homologous recombination (Damke, Dhanaraju, Marsin, Radicella, & Rao, 2015; Fukui et al., 2008; Pinto et al., 2005; Wang & Maier, 2017). The reality that distantly related organisms have adapted their genetic repertoire inherited from the most recent common ancestor would seem obvious. Still, a major thrust of biological exploration is often to examine processes that are highly conserved. While well conserved processes are often critical for more organisms, it is the divergent functions that make each organism unique, which is a property of inherent value found throughout nature.

## Materials and Methods

### Bacteriological methods

All *B. subtilis* strains used in this study are isogenic derivatives of PY79 (Youngman, Perkins, & Losick, 1984), and listed in Table S1. Detailed construction of strains, plasmids and a description of oligonucleotides used in this study are provided in the supplemental text. Plasmids and oligonucleotides are listed in Supplemental Tables S2 and S3, respectively. Media used to culture *B. subtilis* include LB (10 g/L NaCl, 10 g/L tryptone, and 5 g/L yeast extract) and $S7_{50}$ minimal media with 2% glucose (1x $S7_{50}$ salts (diluted from 10x $S7_{50}$ salts: 104.7g/L MOPS, 13.2 g/L, ammonium sulfate, 6.8 g/L monobasic potassium phosphate, pH 7.0 adjusted with potassium hydroxide), 1x metals (diluted from 100x metals: 0.2 M $MgCl_2$, 70 mM $CaCl_2$, 5 mM $MnCl_2$, 0.1 mM $ZnCl_2$, 100 μg/mL thiamine-HCl, 2 mM HCl, 0.5 mM $FeCl_3$), 0.1% potassium glutamate, 2% glucose, 40 μg/mL phenylalanine, 40 μg/mL tryptophan). Selection of *B. subtilis* strains was done using spectinomycin (100 μg/mL) or chloramphenicol (5 μg/mL).

### Spot titer and survival assays

Spot titer assays were performed as described previously (Burby et al., 2018). Survival assays were performed as previously described (Burby et al., 2018), except cells were treated at a density of $OD_{600}$ = 1 instead of 0.5.

### Microscopy

Strains containing RecA-GFP were grown on LB agar with 100 μg/mL spectinomycin at 30°C overnight. Plates were washed with $S7_{50}$ minimal media with 2% glucose. Cultures of $S7_{50}$ minimal media with 2% glucose and 100 μg/mL spectinomycin were inoculated at an $OD_{600}$ =

0.1 and incubated at 30°C protected from light until an $OD_{600}$ of about 0.3 (about 3.5 hours). Cultures were treated with 5 ng/mL MMC and samples were taken for imaging prior to MMC addition, 45 minutes, 90 minutes, and 180 minutes after MMC addition. The vital membrane stain FM4-64 was added to 2 μg/mL and left at room temperature for five minutes. Samples were transferred to 1% agarose pads containing 1x Spizizen salts as previously described (Burby et al., 2018). Images were captured using an Olympus BX61 microscope using 250 ms exposure times for both FM4-64 (membranes) and GFP. RecA-GFP foci were determined by using the find maxima function in ImageJ with the threshold set to the background of the image by comparing a line trace of an area without cells. The number of cells with foci was determined by taking the total number of foci and subtracting the foci greater than one in cells having multiple foci (*i.e.*, if a cell had two foci, one would be subtracted and if a cell had 3 foci two would be subtracted and so on). The percentage was determined by dividing the number of cells with a focus or foci by the total number of cells observed.

**DNA crosslinking assay**

Strains of *B. subtilis* were struck out on LB agar and incubated at 30°C overnight. Plates were washed with LB and samples of 0.5 mL $OD_{600}$ = 3 were aliquoted. One sample was untreated and three samples were treated with 1 μg/mL MMC. Samples were incubated at 37°C for 1 hour. For the untreated and MMC treatment samples, one volume (0.5 mL) of methanol was added and samples were mixed by inversion. Samples were harvested via centrifugation (12,000 *g* for 5 minutes, washed twice with 0.5 mL 1x PBS pH 7.4 and stored at -20°C overnight). For recovery samples, cells from the remaining two treated samples were pelleted via centrifugation (10,000 *g* for 5 minutes) washed twice with 1 mL LB media and then re-suspended in 0.6 mL LB media. Samples were then transferred to 14 mL round bottom culture tubes and incubated at 37°C on a rolling rack for 45 or 90 minutes. An equal volume (0.6 mL) of methanol was added and samples were mixed by inversion. Samples were harvested as stated above and stored at -20°C overnight. Chromosomal DNA was extracted using a silica spin-column as previously described (Burby et al., 2018). Samples were normalized by $A_{260}$ to 15 ng/μL. Samples were heat denatured by incubating at 100°C for 6 minutes followed by placing directly into an ice-water bath for 5 minutes. For native samples and heat denatured samples, 300 ng and 600 ng, respectively, were loaded onto a 0.8% agarose gel with ethidium bromide and electrophoresed at 90 volts for

approximately one hour. The crosslinked species was quantified in gels from two independent experiments in ImageJ. The intensity of the crosslinked band was determined using the Gel Analyzer tool, and the background from the region above the crosslinked band was subtracted and the difference was normalized to the intensity of the native chromosomal DNA band (Fig 5A, lower panel). The average of two independent experiments is shown, with error bars representing the range of the two measurements.

**Bacterial two-hybrid assays**

Bacterial two-hybrid assays were performed as described (Burby et al., 2018; Karimova et al., 2017).

**MrfB protein purification**

MrfB was purified from *E. coli* cells as follows. 10xHis-Smt3-MrfB was expressed from plasmid pPB97 in *E. coli* NiCo21 cells (NEB) at 37°C. Cells were pelleted and resuspended in lysis buffer (50 mM Tris pH7.5, 300 mM NaCl, 5% sucrose, 25 mM imidazole, 1x Roche protease inhibitor cocktail). Cells were lysed via sonication and lysates were clarified via centrifugation: 18,000 rpm (Sorvall SS-34 rotor) for 45 minutes at 4°C. Clarified lysates were loaded onto $Ni^{2+}$-NTA-agarose pre-equilibrated in lysis buffer in a gravity column. The column was washed with 25 column volumes wash buffer (50 mM Tris pH 7.5, 500 mM NaCl, 10% (v/v) glycerol, 40 mM imidazole). MrfB was eluted from the column by cleavage of the 10xHis-Smt3 tag using 6xHis-Ulp1 in 10 column volumes of digestion buffer (50 mM Tris pH 7.5, 150 mM NaCl, 10% glycerol, 10 mM imidazole, 1 mM DTT, and 20 μg/mL 6xHis-Ulp1) at room temperature for 150 minutes. The eluate containing untagged MrfB was collected as the flow through. MrfB was concentrated using a 10 kDa Amicon centrifugal filter. MrfB was loaded onto a HiLoad superdex 200-PG 16/60 column pre-equilibrated with gel filtration buffer (50 mM Tris pH 7.5, 250 mM NaCl, and 5% (v/v) glycerol). The column was eluted with gel filtration buffer at a flow rate of 1 mL/min. Peak fractions were pooled, glycerol was added to a final concentration of 20%, and concentrated using a 10 kDa Amicon centrifugal filter. MrfB aliquots were frozen at a final concentration of 2.6 μM in liquid nitrogen, and stored at 80°C.

**Exonuclease assays**

Exonuclease reactions (20 μL) were performed in 25 mM Tris pH 7.5, 20 mM KCl, and 5 mM $MgCl_2$ as indicated in the figure legends. The plasmid pUC19 was used as a substrate at a concentration of 13.5 ng/μL. To generate linear or nicked substrate, pUC19 was first incubated with BamHI-HF (NEB) or Nt.BSPQ1 (NEB), respectively, for 30 minutes at 37°C. To test metal dependency of MrfB, the linearized pUC19 was purified using a silica spin-column. Reactions were initiated by adding MrfB to 130 nM, 10 units of $T_5$ exonuclease (NEB), or 5 units of λ exonuclease (NEB) and incubating at 37°C as indicated in the figure legends. Reactions were terminated by the addition of 8 μL of nuclease stop buffer (50% glycerol and 100 mM EDTA) followed by resolving reaction products by agarose gel electrophoresis.

**Phylogenetic analysis**

The protein sequences of MrfA (AHA78094.1) and MrfB (AHA78093.1) were used in a PSI-BLAST search in the organisms listed in Table S4. If a putative homolog was detected, the coverage and percent identity were both recorded (Table S4). For MrfA, the protein was considered a homolog if the DEXH helicase domain, the C-terminal domain, and the four conserved cysteines were all present. For MrfB, the protein was considered a homolog if the putative catalytic residues were conserved.

**Acknowledgements**

PEB was supported by a predoctoral fellowship #DGE1256260 from the National Science Foundation. National Institutes of Health grant R01 GM107312 to LAS supported this work. The authors have no conflict of interest to declare.

**Author contributions**

This study was conceived and designed by P.E.B. and L.A.S. Experiments were performed by P.E.B. Data analysis was performed by P.E.B and L.A.S. The manuscript was written and revised by P.E.B. and L.A.S.

## References


Bargonetti, J., Champeil, E., & Tomasz, M. (2010). Differential toxicity of DNA adducts of mitomycin C. *J Nucleic Acids, 2010*. doi:10.4061/2010/698960

Bizanek, R., McGuinness, B. F., Nakanishi, K., & Tomasz, M. (1992). Isolation and structure of an intrastrand cross-link adduct of mitomycin-c and DNA. *Biochemistry, 31*(12), 3084-3091. doi:10.1021/bi00127a008

Bochman, M. L., Paeschke, K., Chan, A., & Zakian, V. A. (2014). Hrq1, a homolog of the human RecQ4 helicase, acts catalytically and structurally to promote genome integrity. *Cell Rep, 6*(2), 346-356. doi:10.1016/j.celrep.2013.12.037

Borowyborowski, H., Lipman, R., Chowdary, D., & Tomasz, M. (1990). Duplex oligodeoxyribonucleotides cross-linked by mitomycin-c at a single site - synthesis, properties, and cross-link reversibility. *Biochemistry, 29*(12), 2992-2999. doi:10.1021/bi00464a015

Borowyborowski, H., Lipman, R., & Tomasz, M. (1990). Recognition between mitomycin-c and specific DNA-sequences for cross-link formation. *Biochemistry, 29*(12), 2999-3006. doi:10.1021/bi00464a016

Burby, P. E., & Simmons, L. A. (2017). MutS2 Promotes Homologous Recombination in Bacillus subtilis. *J Bacteriol, 199*(2). doi:10.1128/jb.00682-16

Burby, P. E., Simmons, Z. W., Schroeder, J. W., & Simmons, L. A. (2018). Discovery of a dual protease mechanism that promotes DNA damage checkpoint recovery. *PLoS Genet, 14*(7), e1007512. doi:10.1371/journal.pgen.1007512

Croteau, D. L., DellaVecchia, M. J., Wang, H., Bienstock, R. J., Melton, M. A., & Van Houten, B. (2006). The C-terminal zinc finger of UvrA does not bind DNA directly but regulates damage-specific DNA binding. *J Biol Chem, 281*(36), 26370-26381. doi:10.1074/jbc.M603093200

Damke, P. P., Dhanaraju, R., Marsin, S., Radicella, J. P., & Rao, D. N. (2015). The nuclease activities of both the Smr domain and an additional LDLK motif are required for an efficient anti-recombination function of Helicobacter pylori MutS2. *Mol Microbiol, 96*(6), 1240-1256. doi:10.1111/mmi.13003

Demain, A. L., & Vaishnav, P. (2011). Natural products for cancer chemotherapy. *Microb Biotechnol, 4*(6), 687-699. doi:10.1111/j.1751-7915.2010.00221.x

Dronkert, M. L., & Kanaar, R. (2001). Repair of DNA interstrand cross-links. *Mutat Res, 486*(4), 217-247.

Edgar, R. C. (2004). MUSCLE: multiple sequence alignment with high accuracy and high throughput. *Nucleic Acids Res, 32*(5), 1792-1797. doi:10.1093/nar/gkh340

Felsenstein, J. (1985). CONFIDENCE LIMITS ON PHYLOGENIES: AN APPROACH USING THE BOOTSTRAP. *Evolution, 39*(4), 783-791. doi:10.1111/j.1558-5646.1985.tb00420.x

Friedberg, E. C., Walker, G. C., Siede, W., Wood, R. D., Schultz, R. A., & Ellenberger, T. (2006). *DNA Repair and Mutagenesis* (2nd ed.). Washington, D.C.: ASM Press.

Fukui, K., Nakagawa, N., Kitamura, Y., Nishida, Y., Masui, R., & Kuramitsu, S. (2008). Crystal structure of MutS2 endonuclease domain and the mechanism of homologous recombination suppression. *J Biol Chem, 283*(48), 33417-33427. doi:10.1074/jbc.M806755200

Grabarczyk, D. B., Silkenat, S., & Kisker, C. (2018). Structural Basis for the Recruitment of Ctf18-RFC to the Replisome. *Structure, 26*(1), 137-144.e133. doi:10.1016/j.str.2017.11.004

Hata, T., Hoshi, T., Kanamori, K., Matsumae, A., Sano, Y., Shima, T., & Sugawara, R. (1956). Mitomycin, a new antibiotic from Streptomyces. I. *J Antibiot (Tokyo), 9*(4), 141-146.

Ivancic-Bace, I., Vlasic, I., Salaj-Smic, E., & Brcic-Kostic, K. (2006). Genetic evidence for the requirement of RecA loading activity in SOS induction after UV irradiation in Escherichia coli. *J Bacteriol, 188*(14), 5024-5032. doi:10.1128/jb.00130-06

Iyer, V. N., & Szybalski, W. (1963). A molecular mechanism of mitomycin action: Linking of complementary DNA strands. *Proc Natl Acad Sci U S A, 50*, 355-362.

Jaciuk, M., Nowak, E., Skowronek, K., Tanska, A., & Nowotny, M. (2011). Structure of UvrA nucleotide excision repair protein in complex with modified DNA. *Nat Struct Mol Biol, 18*(2), 191-197. doi:10.1038/nsmb.1973

Karimova, G., Gauliard, E., Davi, M., Ouellette, S. P., & Ladant, D. (2017). Protein-Protein Interaction: Bacterial Two-Hybrid. *Methods Mol Biol, 1615*, 159-176. doi:10.1007/978-1-4939-7033-9_13

Karimova, G., Pidoux, J., Ullmann, A., & Ladant, D. (1998). A bacterial two-hybrid system based on a reconstituted signal transduction pathway. *Proc Natl Acad Sci U S A, 95*(10), 5752-5756.

549 Kelley, L. A., Mezulis, S., Yates, C. M., Wass, M. N., & Sternberg, M. J. (2015). The Phyre2
550 web portal for protein modeling, prediction and analysis. *Nat Protoc, 10*(6), 845-858.
551 doi:10.1038/nprot.2015.053
552 Kidane, D., & Graumann, P. L. (2005). Dynamic formation of RecA filaments at DNA double
553 strand break repair centers in live cells. *J Cell Biol, 170*(3), 357-366.
554 doi:10.1083/jcb.200412090
555 Kisker, C., Kuper, J., & Van Houten, B. (2013). Prokaryotic Nucleotide Excision Repair. *Cold*
556 *Spring Harbor Perspectives in Biology, 5*(3), 18. doi:10.1101/cshperspect.a012591
557 Kreuzer, K. N. (2013). DNA damage responses in prokaryotes: regulating gene expression,
558 modulating growth patterns, and manipulating replication forks. *Cold Spring Harb*
559 *Perspect Biol, 5*(11), a012674. doi:10.1101/cshperspect.a012674
560 Kumar, S., Lipman, R., & Tomasz, M. (1992). Recognition of specific DNA-sequences by
561 mitomycin-c for alkylation. *Biochemistry, 31*(5), 1399-1407. doi:10.1021/bi00120a016
562 Kumar, S., Stecher, G., & Tamura, K. (2016). MEGA7: Molecular Evolutionary Genetics
563 Analysis Version 7.0 for Bigger Datasets. *Mol Biol Evol, 33*(7), 1870-1874.
564 doi:10.1093/molbev/msw054
565 Kwon, S. H., Choi, D. H., Lee, R., & Bae, S. H. (2012). Saccharomyces cerevisiae Hrq1 requires
566 a long 3'-tailed DNA substrate for helicase activity. *Biochem Biophys Res Commun,*
567 *427*(3), 623-628. doi:10.1016/j.bbrc.2012.09.109
568 Lage, C., Goncalves, S. R., Souza, L. L., de Padula, M., & Leitao, A. C. (2010). Differential
569 survival of Escherichia coli uvrA, uvrB, and uvrC mutants to psoralen plus UV-A
570 (PUVA): Evidence for uncoupled action of nucleotide excision repair to process DNA
571 adducts. *J Photochem Photobiol B, 98*(1), 40-47. doi:10.1016/j.jphotobiol.2009.11.001
572 Lenhart, J. S., Brandes, E. R., Schroeder, J. W., Sorenson, R. J., Showalter, H. D., & Simmons,
573 L. A. (2014). RecO and RecR are necessary for RecA loading in response to DNA
574 damage and replication fork stress. *J Bacteriol, 196*(15), 2851-2860.
575 doi:10.1128/jb.01494-14
576 Lenhart, J. S., Schroeder, J. W., Walsh, B. W., & Simmons, L. A. (2012). DNA repair and
577 genome maintenance in Bacillus subtilis. *Microbiol Mol Biol Rev, 76*(3), 530-564.
578 doi:10.1128/mmbr.05020-11
579 Little, J. W. (1981). Lambda exonuclease. *Gene Amplif Anal, 2*, 135-145.

Moolenaar, G. F., van Rossum-Fikkert, S., van Kesteren, M., & Goosen, N. (2002). Cho, a second endonuclease involved in Escherichia coli nucleotide excision repair. *Proc Natl Acad Sci U S A, 99*(3), 1467-1472. doi:10.1073/pnas.032584099

Nei, M., & Kumar, S. (2000). *Molecular Evolution and Phylogenetics*. New York: Oxford University Press.

Noll, D. M., Mason, T. M., & Miller, P. S. (2006). Formation and repair of interstrand cross-links in DNA. *Chem Rev, 106*(2), 277-301. doi:10.1021/cr040478b

Orren, D. K., & Sancar, A. (1989). The (A)BC excinuclease of Escherichia coli has only the UvrB and UvrC subunits in the incision complex. *Proc Natl Acad Sci U S A, 86*(14), 5237-5241.

Perera, A. V., Mendenhall, J. B., Courcelle, C. T., & Courcelle, J. (2016). Cho Endonuclease Functions during DNA Interstrand Cross-Link Repair in Escherichia coli. *J Bacteriol, 198*(22), 3099-3108. doi:10.1128/jb.00509-16

Petit, C., & Sancar, A. (1999). Nucleotide excision repair: from E. coli to man. *Biochimie, 81*(1-2), 15-25.

Pinto, A. V., Mathieu, A., Marsin, S., Veaute, X., Ielpi, L., Labigne, A., & Radicella, J. P. (2005). Suppression of homologous and homeologous recombination by the bacterial MutS2 protein. *Mol Cell, 17*(1), 113-120. doi:10.1016/j.molcel.2004.11.035

Rogers, C. M., & Bochman, M. L. (2017). Saccharomyces cerevisiae Hrq1 helicase activity is affected by the sequence but not the length of single-stranded DNA. *Biochem Biophys Res Commun, 486*(4), 1116-1121. doi:10.1016/j.bbrc.2017.04.003

Rogers, C. M., Wang, J. C., Noguchi, H., Imasaki, T., Takagi, Y., & Bochman, M. L. (2017). Yeast Hrq1 shares structural and functional homology with the disease-linked human RecQ4 helicase. *Nucleic Acids Res, 45*(9), 5217-5230. doi:10.1093/nar/gkx151

Saitou, N., & Nei, M. (1987). The neighbor-joining method: a new method for reconstructing phylogenetic trees. *Mol Biol Evol, 4*(4), 406-425. doi:10.1093/oxfordjournals.molbev.a040454

Sassanfar, M., & Roberts, J. W. (1990). Nature of the SOS-inducing signal in Escherichia coli. The involvement of DNA replication. *J Mol Biol, 212*(1), 79-96. doi:10.1016/0022-2836(90)90306-7

Sayers, J. R., & Eckstein, F. (1990). Properties of overexpressed phage T5 D15 exonuclease. Similarities with Escherichia coli DNA polymerase I 5'-3' exonuclease. *J Biol Chem, 265*(30), 18311-18317.

Sayers, J. R., & Eckstein, F. (1991). A single-strand specific endonuclease activity copurifies with overexpressed T5 D15 exonuclease. *Nucleic Acids Res, 19*(15), 4127-4132.

Shi, W., Punta, M., Bohon, J., Sauder, J. M., D'Mello, R., Sullivan, M., . . . Chance, M. R. (2011). Characterization of metalloproteins by high-throughput X-ray absorption spectroscopy. *Genome Res, 21*(6), 898-907. doi:10.1101/gr.115097.110

Simmons, L. A., Foti, J. J., Cohen, S. E., & Walker, G. C. (2008). The SOS Regulatory Network. *EcoSal Plus, 2008*. doi:10.1128/ecosalplus.5.4.3

Simmons, L. A., Goranov, A. I., Kobayashi, H., Davies, B. W., Yuan, D. S., Grossman, A. D., & Walker, G. C. (2009). Comparison of responses to double-strand breaks between Escherichia coli and Bacillus subtilis reveals different requirements for SOS induction. *J Bacteriol, 191*(4), 1152-1161. doi:10.1128/jb.01292-08

Simmons, L. A., Grossman, A. D., & Walker, G. C. (2007). Replication is required for the RecA localization response to DNA damage in Bacillus subtilis. *Proc Natl Acad Sci U S A, 104*(4), 1360-1365. doi:10.1073/pnas.0607123104

Stracy, M., Jaciuk, M., Uphoff, S., Kapanidis, A. N., Nowotny, M., Sherratt, D. J., & Zawadzki, P. (2016). Single-molecule imaging of UvrA and UvrB recruitment to DNA lesions in living Escherichia coli. *Nat Commun, 7*, 12568. doi:10.1038/ncomms12568

Tomasz, M. (1995). Mitomycin C: small, fast and deadly (but very selective). *Chem Biol, 2*(9), 575-579.

Tomasz, M., Chowdary, D., Lipman, R., Shimotakahara, S., Veiro, D., Walker, V., & Verdine, G. L. (1986). Reaction of DNA with chemically or enzymatically activated mitomycin-c - isolation and structure of the major covalent adduct. *Proc Natl Acad Sci U S A, 83*(18), 6702-6706. doi:10.1073/pnas.83.18.6702

Tomasz, M., Lipman, R., Chowdary, D., Pawlak, J., Verdine, G. L., & Nakanishi, K. (1987). Isolation and structure of a covalent cross-link adduct between mitomycin C and DNA. *Science, 235*(4793), 1204-1208.

Truglio, J. J., Croteau, D. L., Van Houten, B., & Kisker, C. (2006). Prokaryotic nucleotide excision repair: the UvrABC system. *Chem Rev, 106*(2), 233-252. doi:10.1021/cr040471u

Van Houten, B., Croteau, D. L., DellaVecchia, M. J., Wang, H., & Kisker, C. (2005). 'Close-fitting sleeves': DNA damage recognition by the UvrABC nuclease system. *Mutat Res, 577*(1-2), 92-117. doi:10.1016/j.mrfmmm.2005.03.013

Wang, G., & Maier, R. J. (2017). Molecular basis for the functions of a bacterial MutS2 in DNA repair and recombination. *DNA Repair (Amst), 57*, 161-170. doi:10.1016/j.dnarep.2017.07.004

Warren, A. J., Maccubbin, A. E., & Hamilton, J. W. (1998). Detection of mitomycin C-DNA adducts in vivo by 32P-postlabeling: time course for formation and removal of adducts and biochemical modulation. *Cancer Res, 58*(3), 453-461.

Weng, M. W., Zheng, Y., Jasti, V. P., Champeil, E., Tomasz, M., Wang, Y. S., . . . Tang, M. S. (2010). Repair of mitomycin C mono- and interstrand cross-linked DNA adducts by UvrABC: a new model. *Nucleic Acids Res, 38*(20), 6976-6984. doi:10.1093/nar/gkq576

Yakovleva, L., & Shuman, S. (2012). Mycobacterium smegmatis SftH exemplifies a distinctive clade of superfamily II DNA-dependent ATPases with 3' to 5' translocase and helicase activities. *Nucleic Acids Res, 40*(15), 7465-7475. doi:10.1093/nar/gks417

Yang, W. (2011). Nucleases: diversity of structure, function and mechanism. *Q Rev Biophys, 44*(1), 1-93. doi:10.1017/s0033583510000181

Youngman, P., Perkins, J. B., & Losick, R. (1984). Construction of a cloning site near one end of TN917 into which foreign DNA may be inserted without affecting transposition in Bacillus subtilis or expression of the transposon-bourne ERM gene. *Plasmid, 12*(1), 1-9. doi:10.1016/0147-619x(84)90061-1

## Figure legends

**Figure 1. DNA damage sensitivity of Δ*mrfAB* is specific to mitomycin C. (A)** Relative fitness plots for the indicated gene disruptions from Tn-seq experiments previously reported (Burby et al., 2018). The mean fitness is plotted as a bar graph and the error bars represent the 95% confidence interval. **(B)** Spot titer assay using strains with the indicated genotypes grown on LB with the indicated supplements. **(C)** Spot titer assay using strains with the indicated genotypes grown on LB media with the indicated treatments. For UV irradiation, cells were exposed to the

indicated dose after serial dilutions were spotted on plates. For trioxsalen plates, 1 μg/mL was used and the UV wavelength for irradiation was 365 nm.

**Figure 2. MrfA and MrfB function in the same pathway. (A)** Spot titer assay using strains with the indicated genotypes grown on the indicated media. **(B)** Bacterial two-hybrid assay using the indicated T18 and T25 fusions. **(C)** MrfA constructs used in deletion analysis of MrfA-MrfB interaction (upper) and a bacterial two-hybrid assay using T25-MrfB and the indicated MrfA-T18 fusions (lower). **(D)** MrfB constructs used in deletion analysis of MrfA-MrfB interaction (upper) and a bacterial two-hybrid assay using MrfA-T18 and the indicated T25-MrfB fusions (lower).

**Figure 3. MrfB is a metal-dependent exonuclease. (A)** A schematic of MrfB depicting putative catalytic residues and C-terminal tetratrichopeptide repeat (TPR) domain. **(B)** Spot titer assay using strains with the indicated genotypes spotted on the indicated media. **(C)** 1 μg of purified MrfB stained with Coomassie brilliant blue. **(D)** Exonuclease assay using pUC19 linearized with BamHI (lanes 3-7). Reactions were incubated at 37°C for 15 minutes with or without MrfB, $MgCl_2$, or EDTA as indicated, and separated on an agarose gel stained with ethidium bromide. Lane 1 is a 1 kb plus molecular weight marker (M) and lane 2 is undigested pUC19 plasmid. **(E)** Exonuclease assay testing substrate preference. The indicated exonucleases were incubated with a closed covalent circular plasmid (CCC), a nicked plasmid (Nicked) or a linear plasmid (Linear) in the presence of $Mg^{2+}$ at 37°C for 10 minutes. Reaction products were separated on an agarose gel stained with ethidium bromide. Lane 1 is a 1 kb plus molecular weight marker (M).

**Figure 4. MrfAB function independent of UvrABC dependent nucleotide excision repair. (A & B)** Spot titer assays using strains with the indicated genotypes grown on the indicated media. **(C)** Survival assay using strains with the indicated genotypes. The y-axis is the percent survival relative to the untreated (0 ng/mL) condition. The x-axis indicates the concentration of MMC used for a 30 minute acute exposure. The data points represent the mean of three independent experiments performed in triplicate (n=9) ± SEM.

**Figure 5. MrfAB are not required for unhooking inter-strand DNA crosslinks. (A)** DNA crosslinking repair assay. Chromosomal DNA from untreated samples (U), 1 μg/mL MMC treated samples (T), and recovery samples (45’ and 90’) were heat denatured and snap cooled

(upper) or native chromosomal DNA (lower) was separated on an agarose gel stained with ethidium bromide. A 1 kb plus molecular weight marker is shown in the first lane. **(B)** A bar graph showing the mean percent of crosslinked DNA (see methods) from two independent experiments, and error bars represent the range of the two measurements.

**Figure 6. MrfAB and UvrABC are required for efficient RecA-GFP focus formation. (A)** Representative micrographs of strains containing RecA-GFP expressed from the native locus in addition to the indicated genotypes. Images were captured at the indicated times following MMC addition (5 ng/mL). RecA-GFP is shown in green and the merged images show RecA-GFP (green) and membranes stained with FM4-64 (red). The white bar indicates 5 µm **(B)** Percentage of cells with a RecA-GFP focus or foci over the indicated time course of MMC treatment (5 ng/mL). The error bars represent the 95% confidence interval.

**Figure 7. MrfAB are conserved in diverse bacterial *phyla*. (A)** A rooted phylogenetic tree constructed using 16s rRNA sequences (18s rRNA for *S. cerevisiae*), aligned with muscle (Edgar, 2004), using the neighbor joining method (Saitou & Nei, 1987), and the evolutionary distances were calculated using the p-distance method (Nei & Kumar, 2000). The percentage of replicate trees that resulted in the associated species clustering together in a bootstrap test (500 replicates) is indicated next to the branches (Felsenstein, 1985). Evolutionary analysis was performed in MEGA (Kumar, Stecher, & Tamura, 2016). *In this organism MrfA and MrfB homologs are fused into a single protein. **(B)** Spot titer assay using codon optimized versions of MrfA and MrfB from the indicated species to complement Δ*mrfA* (upper) or Δ*mrfB* (lower).

**Figure 8. A model for MrfAB mediated nucleotide excision repair.** We propose that either an unknown factor or MrfA recognizes an MMC adduct. MrfB is then recruited, and MrfA uses its helicase activity to separate the strand containing the MMC adduct, facilitating MrfB-dependent degradation of the adduct containing DNA. The source of the nick used to direct excision is unknown.

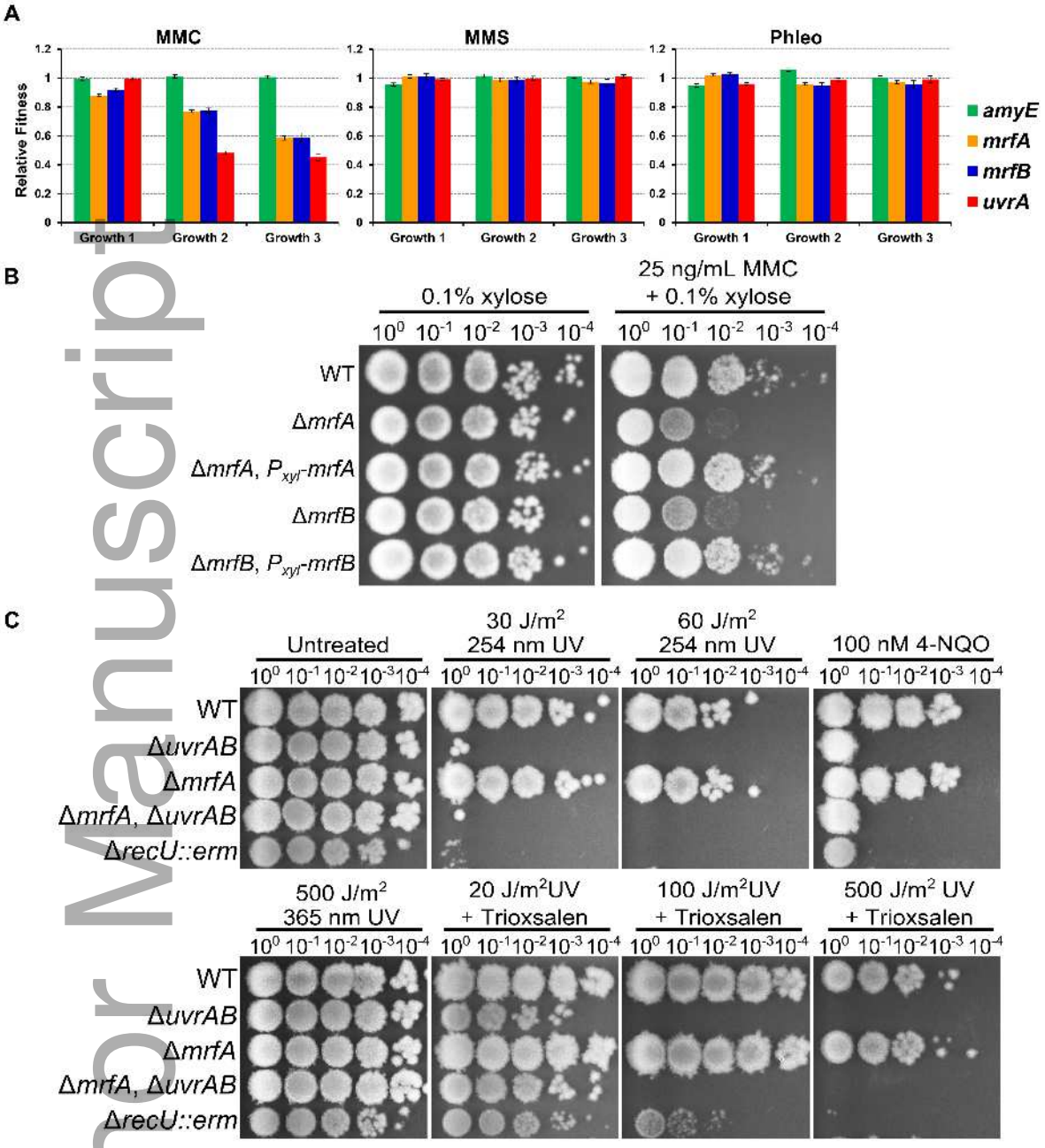


mmi_14158_f1.tif

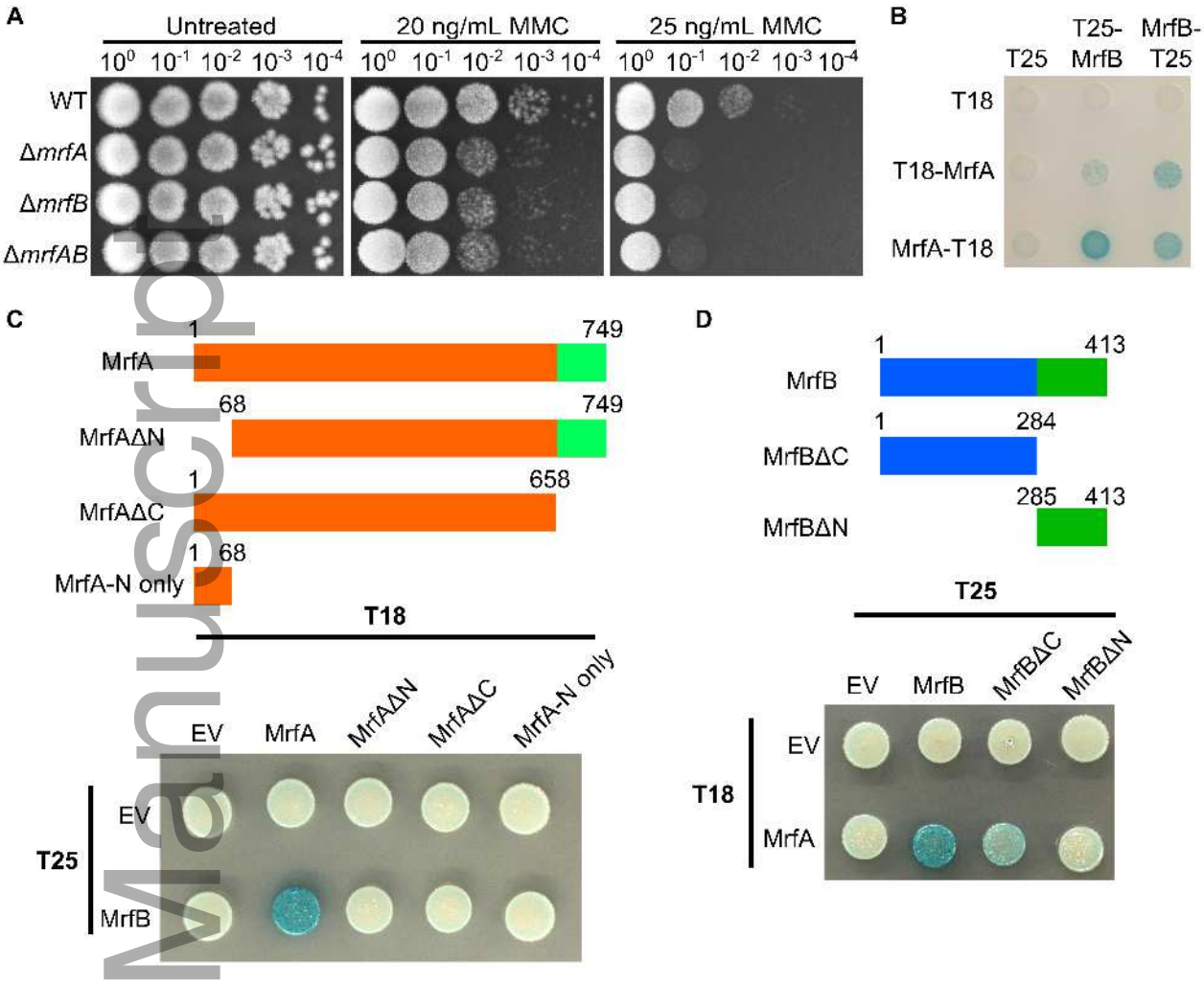


mmi_14158_f2.tif

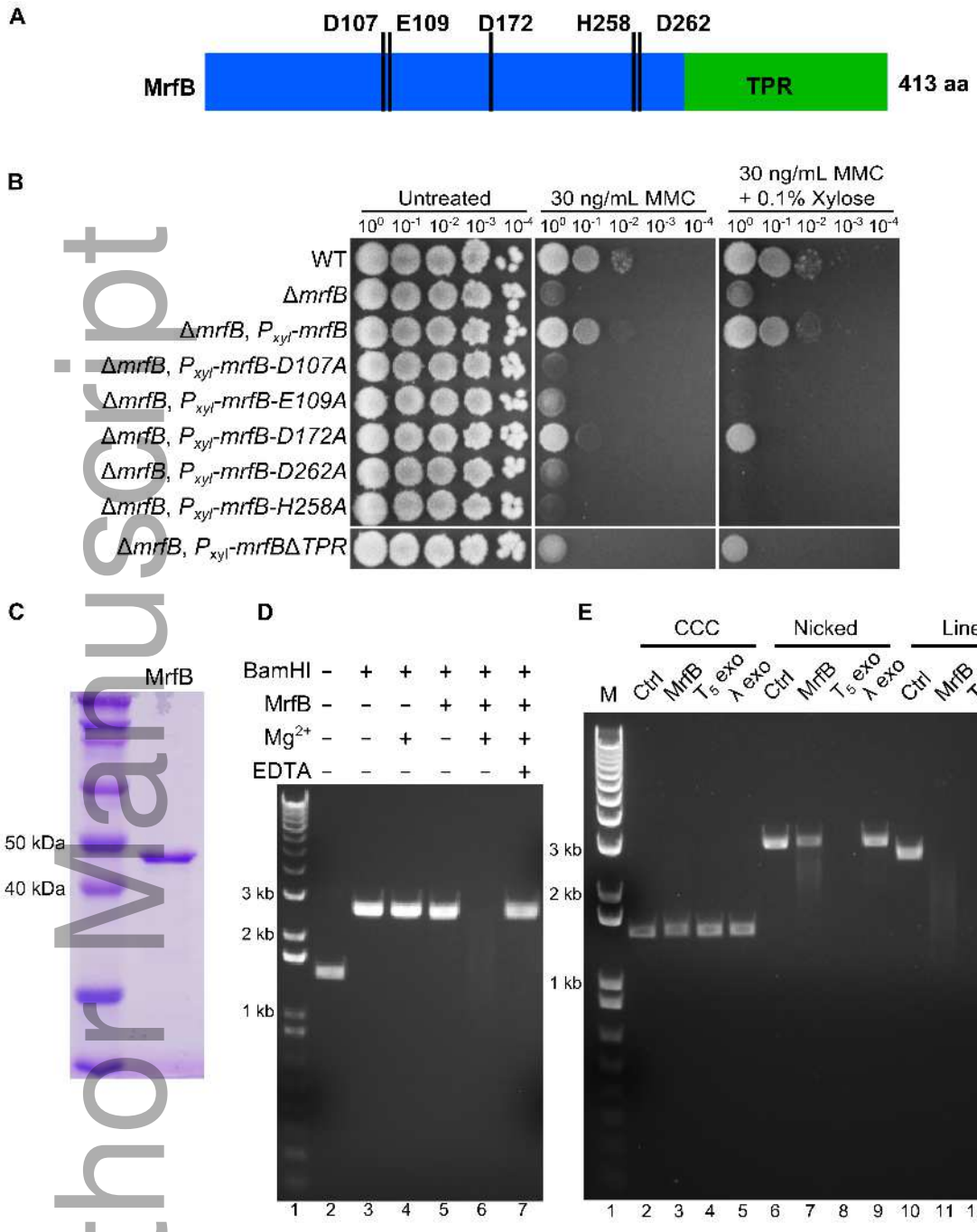


mmi_14158_f3.tif

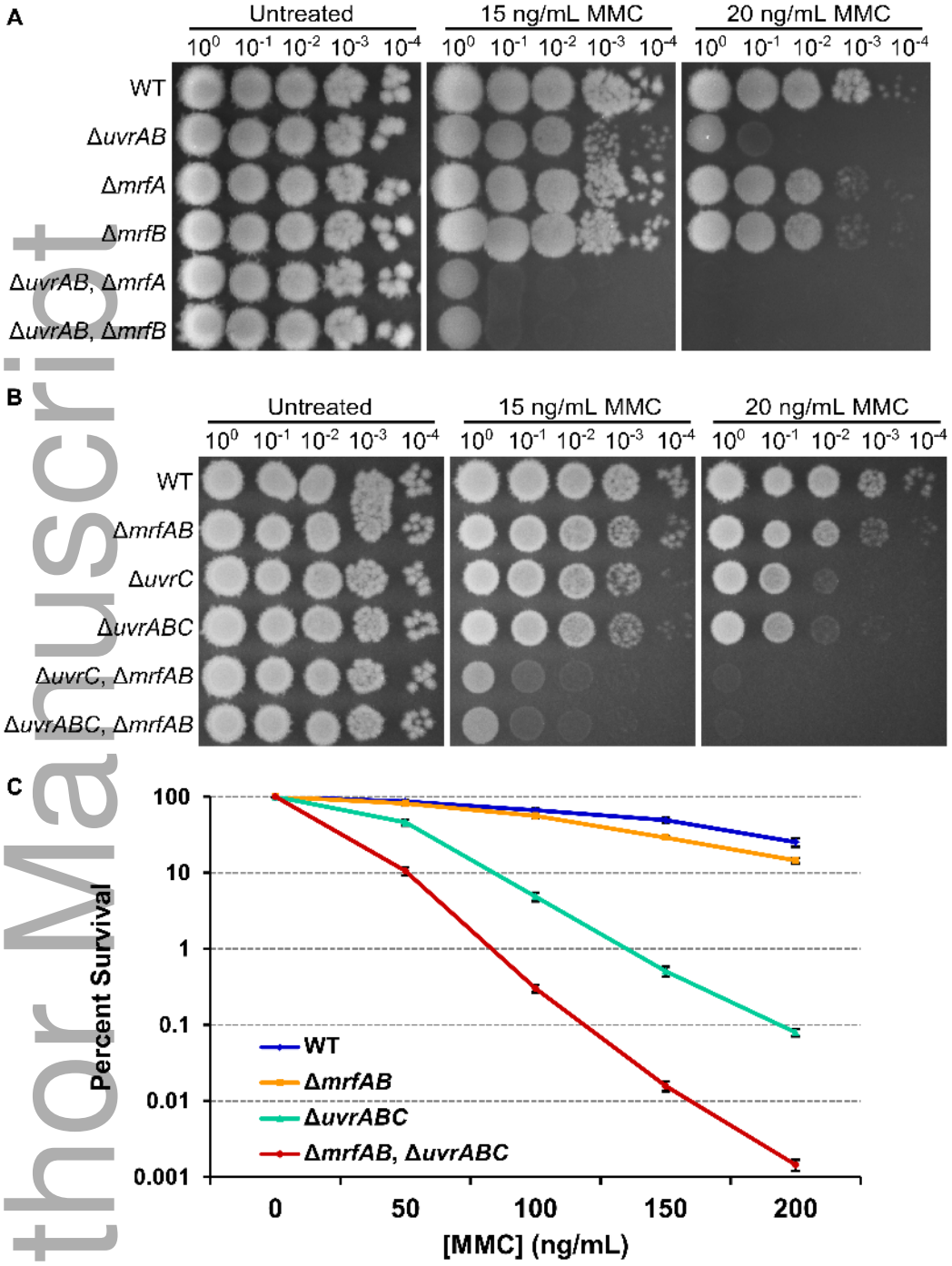


mmi_14158_f4.tif

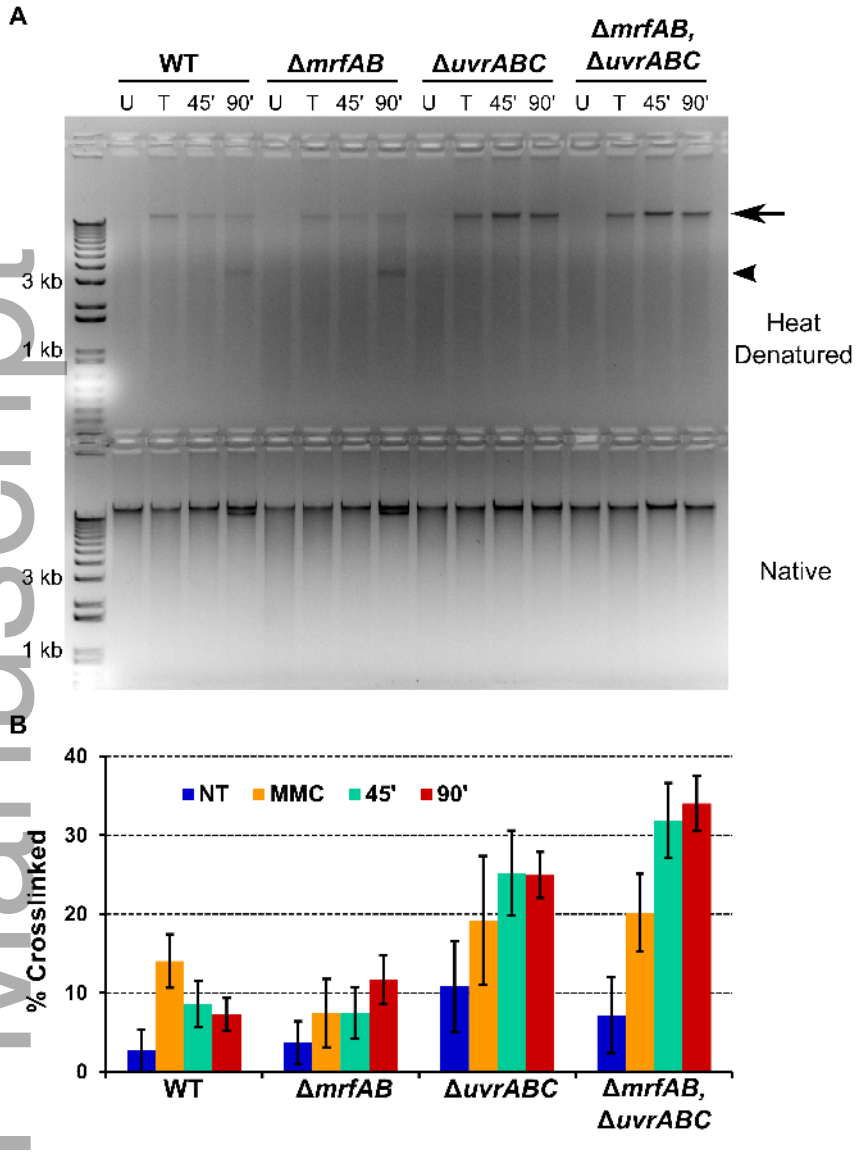


mmi_14158_f5.tif

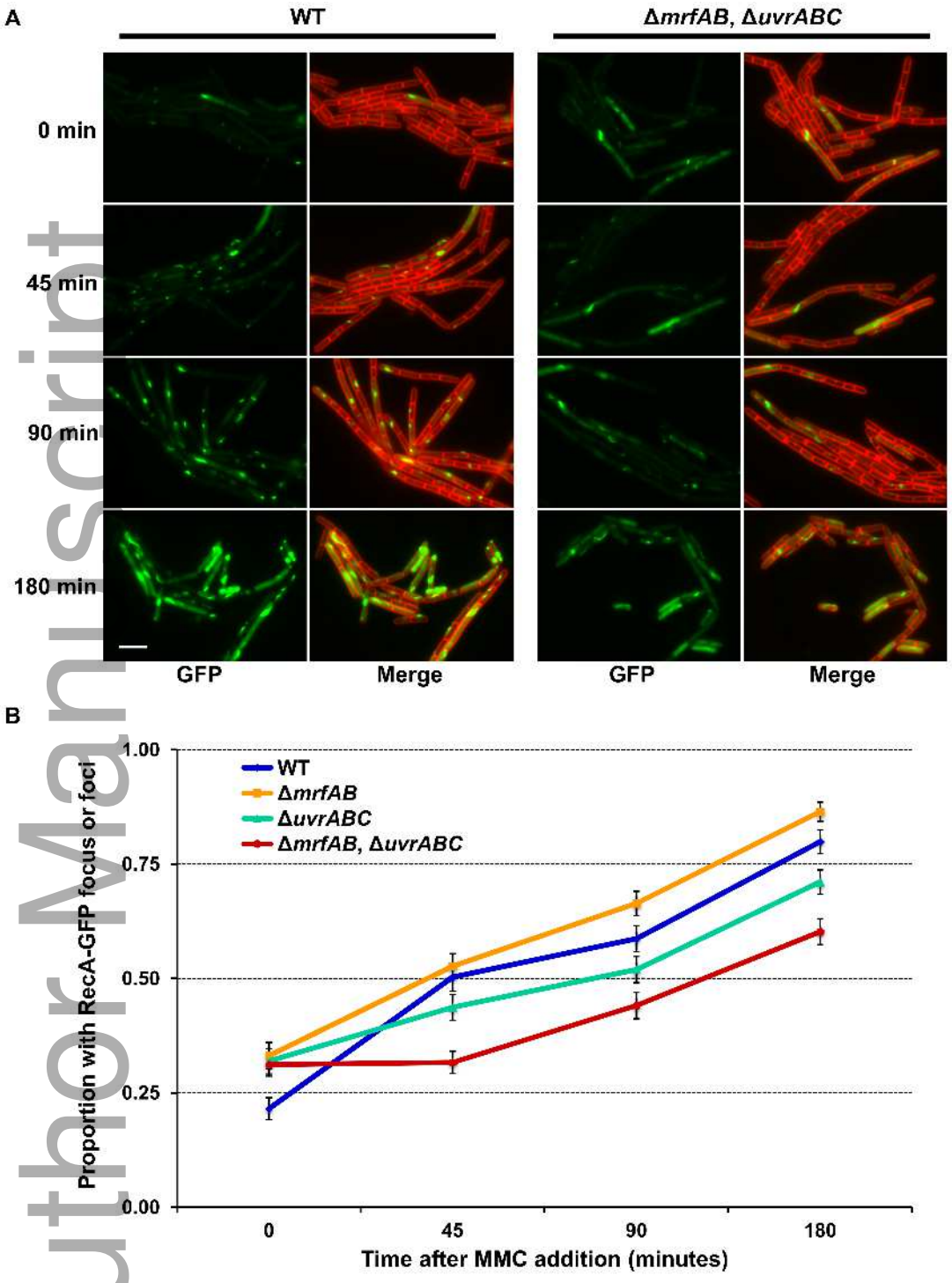


mmi_14158_f6.tif

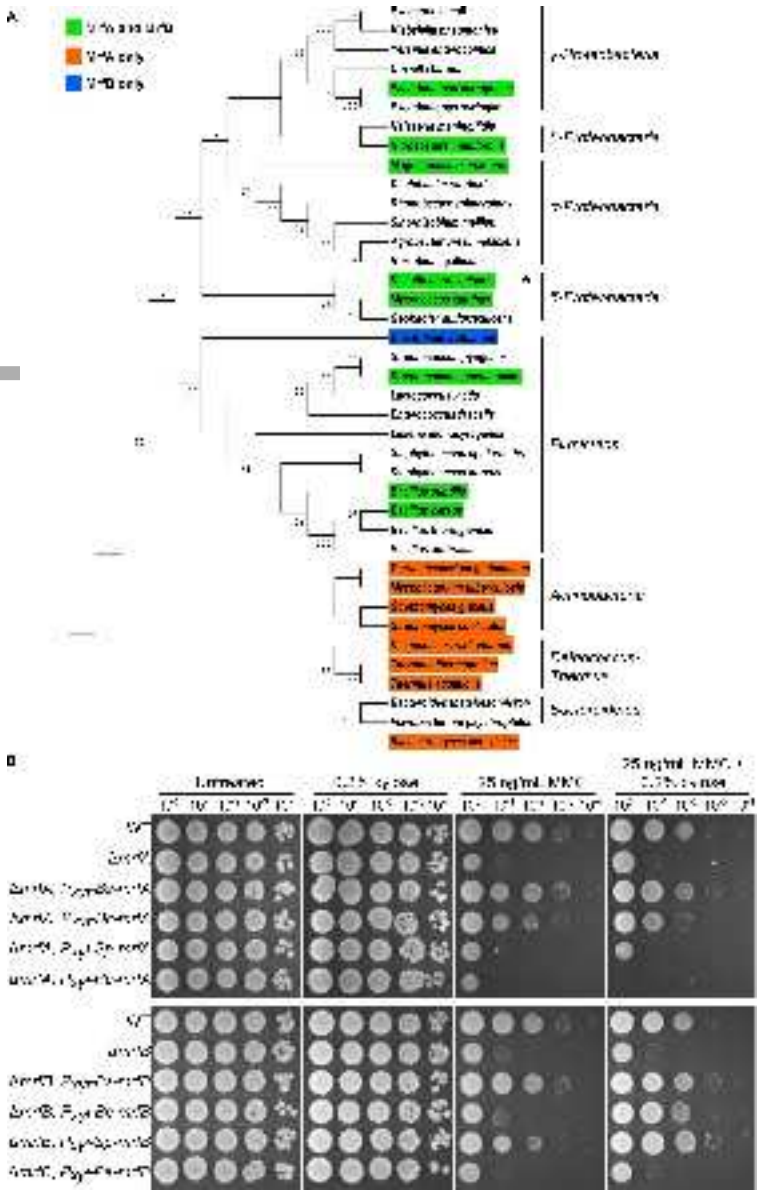

mmi_14158_f7.tif

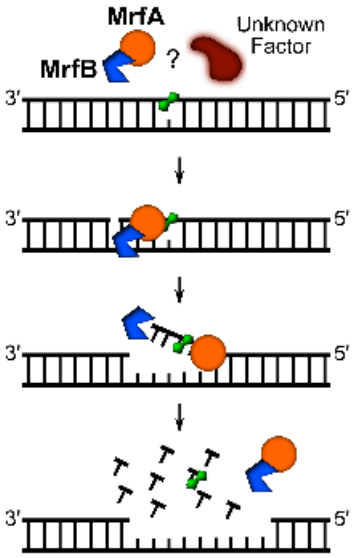


mmi_14158_f8.tif